Accuracy of Eigenvalue Obtained with Hybrid Elements on Axisymmetric Domains

Yoshihisa Iwashita
Nuclear Science Research Facility, Inst. for Chem. Res., Kyoto University, Gokanosho, Uji, Kyoto 611, JAPAN

Abstract—**Eigenvalues of dipole modes in a cylindrical cavity and a spherical cavity were calculated with hybrid triangular elements assuming the sin $m\theta$ and cos $m\theta$ dependencies of the field, and compared with their analytical values. The elements are a combination of linear edge elements for r- and z-components and quadratic nodal elements for the azimuthal one. Because two out of eight degrees of freedom in the linear edge element are internal, they are often omitted. The 14-parameter elements showed a quadratic convergence on mesh refinement, while the 12-parameter ones showed the linear rate like constant edge elements.**

Index terms—**Cavity, Eigenvalues, Electromagnetic fields, Finite element methods.**

I. INTRODUCTION

Higher-order hybrid triangular elements provide accurate numerical solutions with shorter CPU time. The elements are a combination of linear edge elements for r- and z-components and quadratic nodal elements for the azimuthal one. Fig. 1 shows the shape functions for second order elements as well as lowest order elements. The bottom two functions represent the internal degrees of freedom, which are omitted in some applications. In order to provide a numerical solution of an Eigenvalue problem in cylindrical coordinate systems, vector finite element methods with hybrid elements were formulated [1],[2]. This paper compares the accuracy of these elements for Eigenvalue problems.

II. FORMULATION

Because either $\vec{E}$ or $\vec{H}$ can be used as the field variable, only the electric field will be shown here. The differential equations to be solved are [3],[4],[5],

$$\nabla\times\nabla\times\vec{E}+k^2\vec{E}=\vec{0},\quad \nabla\cdot\vec{E}=\vec{0}\qquad (in\quad \Omega), \tag{1}$$

where $k^2=\omega^2\varepsilon\mu$. In vacuum space $k^2=\omega^2/c^2$, where c is the speed of light. Boundary conditions are

$$\vec{E}\cdot\vec{n}=0 \quad \text{on magnetic boundaries } (\Gamma m) \tag{2}$$

$$\vec{E}\times\vec{n}=\vec{0} \quad \text{on electric boundaries } (\Gamma e) \text{ and} \tag{3}$$

$$\vec{E}_{left}=e^{i\varphi}\vec{E}_{right} \quad \text{on periodic ones } (\Gamma p), \tag{4}$$

where $\vec{n}$ denotes the outward normal on the boundary, and φ is the phase advance in the problem (6). Integrating (1) over Ω after multiplying by $\delta\vec{E}$ (virtual electric field), we get

$$\int_\Omega \delta\vec{E}\cdot\nabla\times\nabla\times\vec{E}\,dv=-k^2\int_\Omega \delta\vec{E}\cdot\vec{E}\,dv, \tag{5}$$

and applying Green's theorem, the following relations must hold for any $\delta\vec{E}$:

Manuscript received November 3, 1997.
Y. Iwashita, (81)774-38-3282, fax (81)774-38-3289, iwashita@kyticr.kuicr.kyoto-u.ac.jp, http://wwwal.kuicr.kyoto-u.ac.jp.

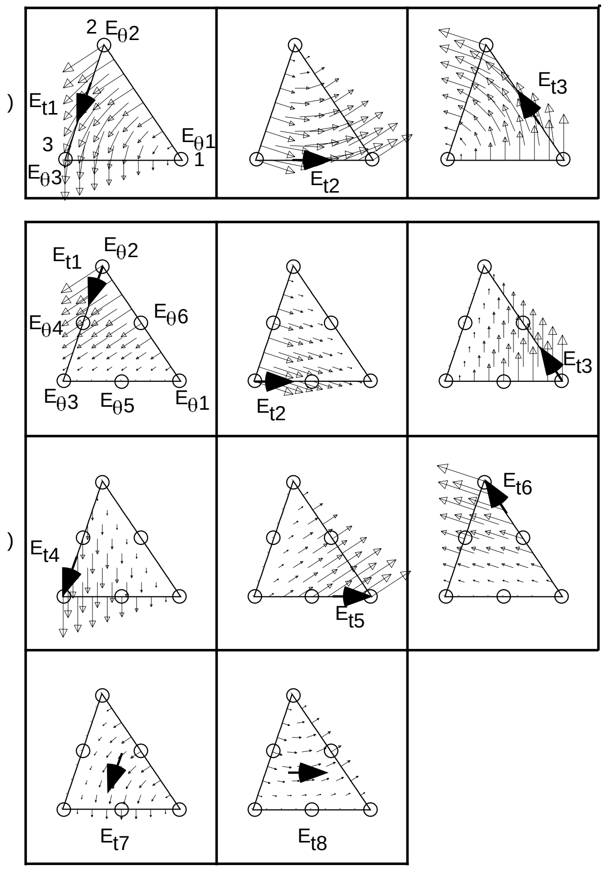

Fig. 1. Hybrid triangular elements.
a) Constant edge and linear nodal elements.
b) Linear edge and quadratic elements. The bottom two shape functions represent the internal freedoms.

$$\oint_\Gamma\left(\nabla\times\vec{E}\right)\times\delta\vec{E}\,d\vec{s}-\int_\Omega\left(\nabla\times\vec{E}\right)\cdot\left(\nabla\times\delta\vec{E}\right)dv=-k^2\int_\Omega\delta\vec{E}\cdot\vec{E}\,dv \tag{6}$$

$$\vec{E}\times\vec{n}=0 \text{ and } \delta\vec{E}\times\vec{n}=0 \text{ on } (\Gamma e), \text{ or}$$
$$\vec{E}\cdot\vec{n}=0 \text{ and } \delta\vec{E}\cdot\vec{n}=0 \text{ on } (\Gamma m) \tag{7}$$

The term in the surface integration of (6) becomes zero on either (Γe) or (Γm) because of the boundary condition of (7).

III. FINITE ELEMENT MODEL

Because only the problems on axisymmetric domains are considered, we can assume sin $m\theta$ and cos $m\theta$ dependencies for E_r, E_z and E_θ components, and then the problem can be reduced to two-dimensional problem:

$$\vec{E}=(E_\theta\sin m\theta,\ E_r\cos m\theta,\ E_z\cos m\theta). \tag{8}$$

Then (E_θ, E_r, E_z) are functions of r and z only. The field variables are (rE_θ, E_r, E_z) for $m\geq1$ and (E_θ, H_θ) for m=0. Only the case for $m\geq1$ will be discussed here.

The shape functions used are the hybrid triangular elements of the lowest or the second order with curved boundaries. The lowest one has six parameters, while the second one has twelve or fourteen parameters. The edge element represents the vector components (E_r, E_z) and the nodal element represents the component E_θ.

Then, $\vec{E}$ and $\nabla\times\vec{E}$ can be written as

$$\vec{E}=\begin{bmatrix}E_\theta\\E_r\\E_z\end{bmatrix}=N\cdot\begin{bmatrix}r\vec{E}_\theta\\\vec{E}_t\end{bmatrix},\qquad \nabla\times\vec{E}=N'\cdot\begin{bmatrix}r\vec{E}_\theta\\\vec{E}_t\end{bmatrix}, \tag{9}$$

$$N=\begin{bmatrix}\frac{1}{r}\vec{N}_\theta & \vec{0}\\ \vec{0} & \vec{N}_r\\ \vec{0} & \vec{N}_z\end{bmatrix},\qquad N'=\begin{bmatrix}\vec{0} & \partial_z\vec{N}_r-\partial_r\vec{N}_z\\ \frac{-1}{r}\partial_z\vec{N}_\theta & \frac{-m}{r}\vec{N}_z\\ \frac{1}{r}\partial_r\vec{N}_\theta & \frac{m}{r}\vec{N}_r\end{bmatrix}, \tag{10}$$

where $\vec{N}_\theta$, $\vec{N}_z$, and $\vec{N}_r$ are the shape functions, and $r\vec{E}_\theta$ and $\vec{E}_t$ are the field variables. The base shape functions in (u-v) plane are given in Table I. The last two functions in $\vec{N}_z$, and $\vec{N}_r$ represent the internal freedoms and are omitted in twelve-parameter shape function. The element matrix equation is

$$\int_e N'^{\mathrm{T}}\cdot N'\, r\,dr\,dz=k^2\int_e N^{\mathrm{T}}\cdot N\, r\,dr\,dz\,, \tag{11}$$

where symbol e denotes the element volume. The base shape function is mapped onto a curved boundary element by quadratic coordinate transformation. The integrations are performed numerically up to nineteenth order precision. The singularity in the integrand on the axis is not serious, because the real divergent terms are substituted by the boundary condition on the axis. By assembling all element matrices and applying the boundary condition, finally we get the general Eigenvalue equation:

$$\boldsymbol{M}\cdot\vec{x}=k^2\boldsymbol{K}\cdot\vec{x}\,, \tag{12}$$

TABLE I
SHAPE FUNCTIONS

The lowest order (Constant edge and linear nodal):
$\vec{N}_\theta=[u\;\;v\;\;w]$
$\vec{N}_r=\frac{1}{2A_e}[l_1(v\partial_r w-w\partial_r v)\;\;l_2(w\partial_r u-u\partial_r w)\;\;l_3(u\partial_r v-v\partial_r u)]$
$\vec{N}_z=\frac{1}{2A_e}[l_1(v\partial_z w-w\partial_z v)\;\;l_2(w\partial_z u-u\partial_z w)\;\;l_3(u\partial_z v-v\partial_z u)]$
The second order (Linear edge and quadratic nodal):
$\vec{N}_\theta=[u(2u-1)\;\;v(2v-1)\;\;w(2w-1)\;\;4vw\;\;4wu\;\;4uv]$
$\vec{N}_r=\frac{1}{2A_e}[l_1v\partial_r w\;\;l_2w\partial_r u\;\;l_3u\partial_r v\;\;-l_1w\partial_r v\;\;-l_2u\partial_r w\;\;-l_3v\partial_r u\;\;l_1u(v\partial_r w-w\partial_r v)\;\;l_2v(w\partial_r u-u\partial_r w)]$
$\vec{N}_z=\frac{1}{2A_e}[l_1v\partial_z w\;\;l_2w\partial_z u\;\;l_3u\partial_z v\;\;-l_1w\partial_z v\;\;-l_2u\partial_z w\;\;-l_3v\partial_z u\;\;l_1u(v\partial_z w-w\partial_z v)\;\;l_2v(w\partial_z u-u\partial_z w)]$

where u, v and w are the area coordinates and l_i is the length of the edge facing to the vertex i.

where $\boldsymbol{M}$ and $\boldsymbol{K}$ are large sparse symmetric matrices, and $\vec{x}$ is an Eigenvector. The signs of the matrix elements that correspond to the tangential components are inverted if the incremental direction of the serial number of the corresponding nodes is not equal to that of the elements. Because of the hybrid elements, any spurious mode has zero-Eigenvalue and is well separated from the real modes. Usually several Eigensolutions starting from the smallest one but zero are of interest. Unfortunately, this Eigenvalue problem has many zero-Eigenvalue solutions, which correspond to the spurious modes, and thus special care should be taken.

IV. General Eigenvalue Solver for Large Sparse Symmetric Matrix with Zero Filtering[7],[8]

Because the system matrices are sparse and symmetric, only the lower half of the nonzero values is stored with their column numbers. The general Eigenvalue solver is based on the subspace method with zero filtering. The algorithm is as follows:

0) Take m initial vectors $\boldsymbol{X}=[\boldsymbol{x}_1\;\;\boldsymbol{x}_2\;\;\cdots\;\;\boldsymbol{x}_m]$ and $M'=M+bK$ (shift Eigenvalues to be positive definite).
1) If zero filter is needed then $\boldsymbol{Y}=\boldsymbol{M}'^{-1}\cdot\boldsymbol{K}\cdot\boldsymbol{X}$, $\boldsymbol{X}=\boldsymbol{X}-b\boldsymbol{Y}$.
2) $\boldsymbol{Z}=\boldsymbol{K}\cdot\boldsymbol{X}$, $\boldsymbol{Y}=\boldsymbol{M}'^{-1}\cdot\boldsymbol{Z}$.
3) $\tilde{\boldsymbol{M}}=\boldsymbol{Y}^{\mathrm{T}}\cdot\boldsymbol{M}'\cdot\boldsymbol{Y}$, $\tilde{\boldsymbol{K}}=\boldsymbol{Y}^{\mathrm{T}}\cdot\boldsymbol{K}\cdot\boldsymbol{Y}$ (Transform to subspace).
4) Solve the small Eigenvalue problem: $\tilde{\boldsymbol{M}}\cdot\boldsymbol{p}_i=d\,\tilde{\boldsymbol{K}}\cdot\boldsymbol{p}_i$ and make $\boldsymbol{P}=[\boldsymbol{p}_1\;\;\boldsymbol{p}_2\;\;\cdots\;\;\boldsymbol{p}_m]$.
5) Return to the original space with $\boldsymbol{X}=\boldsymbol{Y}\cdot\boldsymbol{P}$ and normalize $\boldsymbol{x}_i$'s.
6) Repeat from 1) until it converges.

Once the zero filter operation 1) is performed, all the Eigenvector components having zero Eigenvalue disappear from the iterating vectors until they grow by numerical noise. It depends on the numerical precision of the "zero-Eigenvalue" and the iterative operation. The growing rate can be estimated from the ratio of the highest Eigenvalue to the lowest Eigenvalue, which corresponds to the (original) zero-Eigenvalue. Then the frequency of the zero-filter operation can be evaluated. A growing rate is illustrated as a function of the Eigenvalue in Fig. 2, where the zero-filter is operated

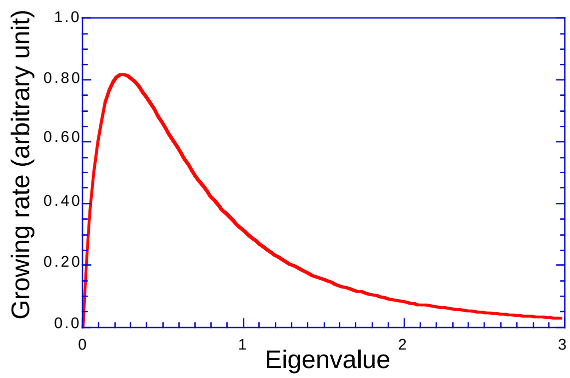

Fig. 2. Growing rate as a function of the Eigenvalue. Zero-filter is operated every four iterations and the shift value is 1.

every four iterations. The positive shift value *b* should be chosen by this consideration for faster and stable convergence. It is usually chosen to be several times larger than the lowest Eigenvalue but zero, which can usually be estimated from the physical size of the cavity.

Because the shift value b is positive, the convergence rate is slower than the conventional negative shift method. It can be improved by similar filtering scheme for higher Eigenvalues. In this point of view, the normal iterative operation is a filter at infinity. After the highest Eigenvalue settles, the convergence is accelerated with filtering points obtained from the roots of the Chebyshev polynomials mapped between the highest Eigenvalue and infinity[9].

V. NUMERICAL RESULT

Numerical calculations for dipole modes (m=1) were performed for a cylindrical cavity with a radius of 10 cm and a length of 10 cm, as well as a spherical cavity with a radius of 10 cm. The boundary conditions of the cylindrical cavity at both ends were tangential electric to include the TE110 mode. The spherical cavity actually was a hemisphere because of the boundary condition. Three kinds of elements described in the previous section were used and compared. The mesh sizes were 0.1, 0.2, 0.5, 1.0, 2.0 and 5.0 cm. Figs. 3 and 4 show the typical mesh for these problems at a mesh size of 1.0 cm. The bottom line corresponds to the axis. The circular boundaries were approximated by quadratic mapping.

Figs. 5 and 6 are the calculated contour plots of rE_θ and arrow plots of (E_z,E_r) for the three lowest modes at mesh

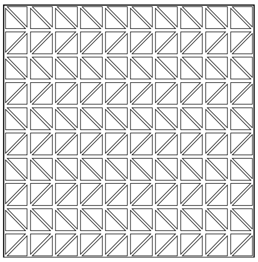

Fig. 3. Mesh plot of the cylindrical cavity. The radius and the length are 10 cm. The mesh size is 1.0 cm.

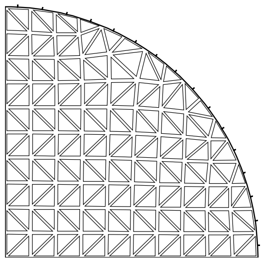

Fig. 4. Mesh plot of the spherical cavity. The radius is 10 cm. The mesh size is 1.0 cm.

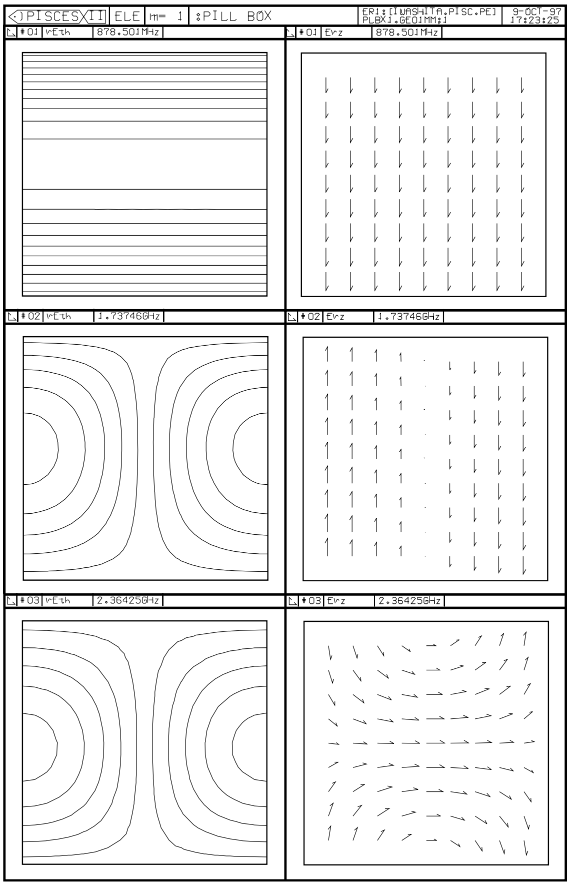

Fig. 5. Contour plots of rE_θ and arrow plots of (E_z,E_r) for the three modes from the lowest in a cylindrical cavity.

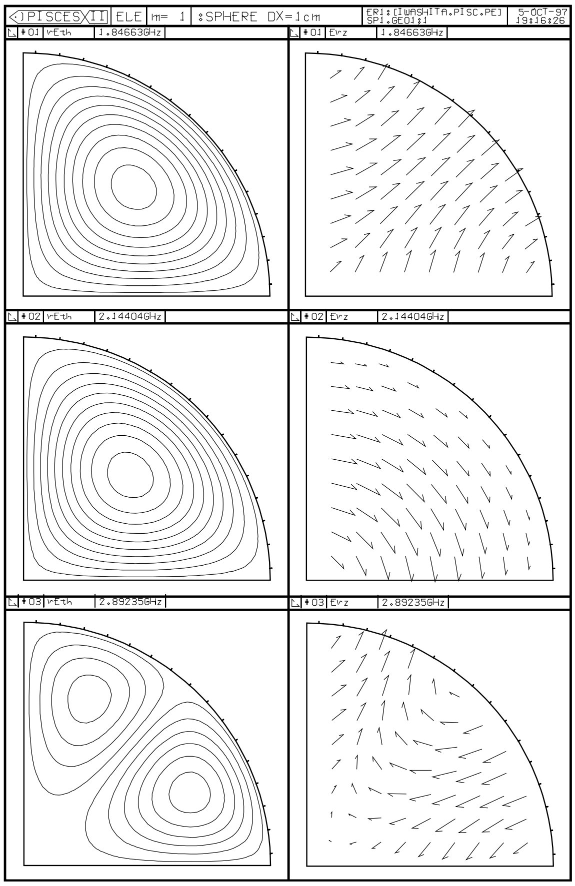

Fig. 6. Contour plots of rE_θ and arrow plots of (E_z,E_r) for the three modes from the lowest in a spherical cavity.

size of 1.0 cm. Because there are sin $m\theta$ and cos $m\theta$ dependencies, the rE_θ plane does not coincide with the (E_z,E_r) plane. The arrows were evaluated at the vertices of all elements and averaged at the merging nodes.

Figs. 7 and 8 show the obtained frequency errors as functions of the number of unknowns. Because the Eigenvalues do not converge from one direction, the frequency errors change their signs and do not decrease monotonously. Although the frequency error decreased with $O(h^2)$ for 14-parameter elements, that for 12-parameter decreased with $O(h)$ except for the TE_{110} mode (lowest mode f_1) in the cylindrical cavity. It may be because the electric field of the TE_{110} mode has no Z-dependence and a small dependence on the r-direction. In such a special case, the internal freedoms may not be necessary for accurate solutions.

VI. Conclusion

The presicions of the Eigenvalues obtained with hybrid elements are compared. For accurate Eigenvalues, the internal freedoms of the linear edge elements seem to be indispensable. Although the internal freedoms slightly increase the computational cost, linear edge elements without them showed the same convergence rate as that of merely constant edge elements even when curved boundaries are applied.

The same situation may arise in a two dimensional problem such as a waveguiding problem.

Acknowledgment

The author would like to thank Drs. M. Hano, E. M. Nelson and T. Higo for their encouragement and useful discussions. He also is greatly indebted to Dr. Maruyama for his helpful information.

References

[1] E. M. Nelson, "A finite element field solver for dipole modes", 1992 Linear Accelerator Conference Proceedings, Ottawa, Ontario, Canada, AECL-10728, Vol2, pp.814-816, August 1992

[2] M. Koshiba, S. Maruyama and K. Hirayama, "A vector finite element method with the high-order mixed-interpolation-type triangular elements for optical waveguiding problems", Journal of Lightwave Technology, Vol.12, No.3, March 1994, pp.495-502.

[3] K. H. Huebner and E. A. Thornton, "The finite element method for engineers", (J.Weiley, New York); and A.R.Mitchell and R.Wait, "The Finite Element Method in Partial Differential Equations" (J.Weiley, New York, 1977)

[4] M. Hara, T. Wada, T.Fukasawa, and F. Kukuchi, "A three dimensional analysis of RF electro-magnetic fields by finite element method", IEEE Trans., MAG-19 No. 6 Nov. 1983

[5] F. Kikuchi et al., "A finite element method for 3-D analysis of cavity resonators", Distributed Parameter Systems: Modeling and Simulation, Elsevier Science Publishers B. V. (North-Holland) ©IMACS,1989

[6] R. L. Gluckstern and E. N. Opp, "Calculation of dispersion curves in periodic structures", IEEE Trans. MAG-21 No. 6 Nov. 1985 pp. 2344-2346

[7] Y. Iwashita, "General Eigenvalue solver for large sparse symmetric matrix with zero filtering", Bull. Inst. Chem. Res. Kyoto Univ. Vol. 67, No. (1989)

[8] Y. Iwashita, "PISCES II:2.5D RF Cavity Code", Computational Accelerator Physics, Williamsburg, VA, AIP conference proceedings No. 361 Sept. 1996, pp.119-124

[9] H. Otsubo and Y. Yamamoto, "Subspace Iteration Accelerated by the Use of Chebyshev Polynomials for Eigenvalue Problems with symmetric Matrices", NAUT Report, No. 4007 (1973)

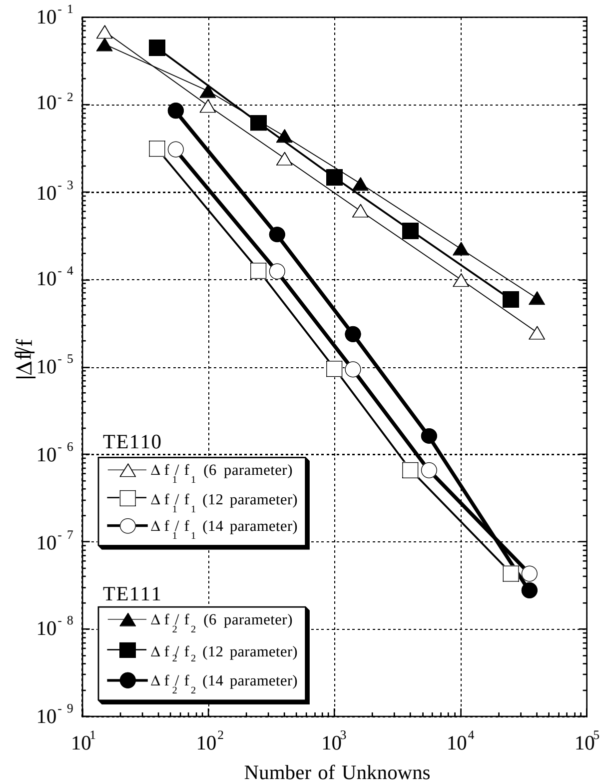

Fig. 7. Relative frequency errors of TE_{110} and TM_{111} modes in a cylindrical cavity as a function of the number of unknowns.

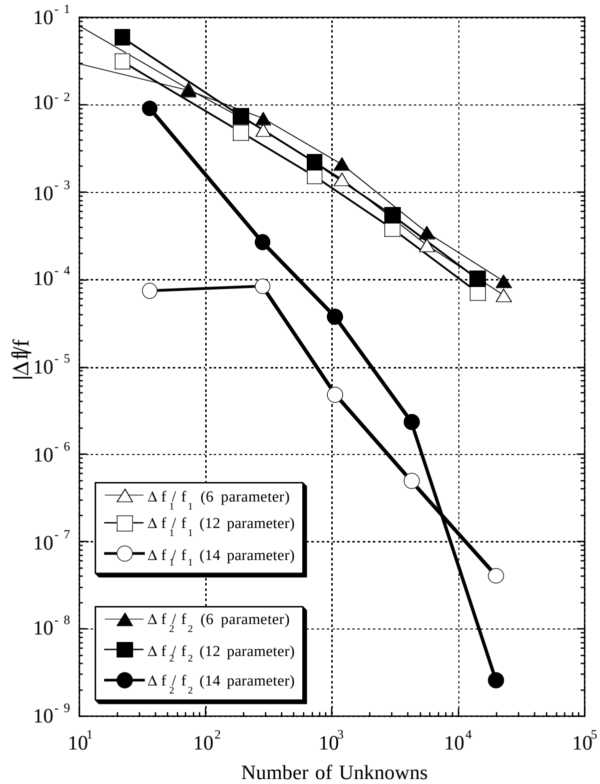

Fig. 8. Relative frequency errors of the second and the third lowest modes in a spherical cavity as a function of the number of unknowns.